Intelligent Instrumented Belaying System in Sports Climbing

Heiko Oppel, Michael Munz
Ulm University of Applied Sciences, Ulm, Germany, heiko.oppel@thu.de, michael.munz@thu.de

Abstract

Sport climbing became a more attractive sport to the broad mass over the last decades. An increasing amount of injuries are the consequences. Inattentiveness and untrained belayer are some of the natural causes. In order to improve their experience, we developed an intelligent belaying system monitoring the belayer during his task to secure the climber throughout his ascent. It is supposed to recognize a climbers' fall if the belayer fails. We specifically designed Machine Learning algorithms in combination with a multi-sensor system for this task. The system is divided in two separate sub-systems, which communicate over wireless LAN protocols in order to keep them synchronized. One of the two sub-systems is integrated into a belay device. It records the movement behavior of the device and the rope running through it. In order to generate label data, the second sub-system was attached onto the climber. Based on the information from the belay device alone, we were able to identify a fall with a certainty of 86.21 %.

1 Introduction

Sport climbing has risen as a popular sport with an increasing community. Inevitably, the amount of injuries grew as well, as a study by Nelson et al. [1] revealed. They surveyed rock climbing injuries which had to be treated in emergency departments in the united states and identified an increase of treatments by 63 % between the years 1990 and 2007. Another study by Schöffl et al. [2] focused on the causes of injuries that occured in a sport climbing gym in Germany over the years 2007 and 2011. Most of their recorded injuries whilst lead or top rope climbing did arise due to a mistake whilst belaying. Within this work we address this deficit in the sport climbing safety control. Therefore, we developed a new multi-sensor system, including an Inertial Measurement Unit (IMU) and Hall-Sensors. They were integrated into an existing belay device. Whereas the IMU is supposed to keep track of the belay devices' movement behaviour, the Hall-Sensors track the rope running through the device. Such a system would benefit as a monitoring system for supporting and training the belayer in critical situations.

Experiments with monitoring systems in sports climbing were already developed and examined in a couple of studies. In contrast to our approach, they rely on systems worn by the climber [3], [4], [5], [6]. Even a study exists on a system worn by the belayer to supervise the severity of a climbers fall [7]. Though, all of those previous studies require an external setup which has to be attached to either the belayer and climber or only the climber to gather the relevant data. Not only is our approach the first one that integrated a monitoring system into a belay device, but it is also the first one that could be used without an additional equipment for climbing.

The idea of this study was to distinguish a fall from other climb specific activities based on the pre-mentioned setup. The first part focuses on the analysis of the recorded data with regard to class separability. We then developed three algorithms to achieve the separation of the two classes. The first one is based on a threshold approach, the second on the Random Forest algorithm. The third method is a combination of the first two approaches.

2 Hardware System

This section provides an overview of the utilized hardware, their configuration and interaction between them. Two hardware systems were developed, one integrated into the belay device and the other was attached to the climber.

2.1 Electronical Hardware for the Belayer

The sensors were integrated into a consisting belay device Eddy from the Edelrid GmbH & Co. KG. This includes three Hall-Sensors interacting with multiple magnets and an Inertial Measurement Unit (IMU), cp. Figure 1 (a). We used three Infineon XENSIV^{TM} magnetic Hall switch TLE4945L sensors [8] which interact with six magnets with varying pole orientations. The magnets were placed into a wheel, which is mechanically pressed against the rope within the belay device. An MPU-9250 from the Infineon company [9] was used to record the movement behavior of the belay device.

Both sensor types were connected to a pre-developed microcontroller by the Adafruit Industries LLC company which comes with a built-in SD-card socket including read/write functionality, cp. Figure 1 (b). That allows to store the raw sensor information on the SD card. Additionally, an ESP8266 from the Espressif Systems company guarantees a wireless communication between climber, belayer and a control software.

2.2 Electronical Hardware for the Climber

This sub-system is supposed to record the required label information for the classification task. Figure 2 shows the

ISBN 978-3-8007-5835-7

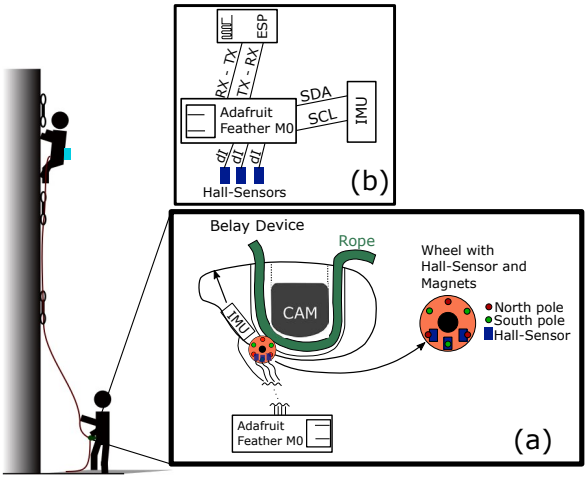

Figure 1 Sketch of the electronical components attached on belayer and belay device. (a): The sensors on the belay device are connected to a circuit board attached to the harness of the belayer. They consist of an IMU and three Hall-Sensors, coming with magnets integrated into a wheel, which is pushed against the rope within the belay device. (b): Visualization of the communication protocols between the sensors and the microcontroller. The IMU send the information via I^2C to the microcontroller, whereas the ESP module communicated over UART. The Hall-Sensors were sending their state to a digitial pin (dI).

electronical parts attached to the climber. They are fixed on the harness of the climber in climb situations or on top of the sandbag in fall scenarios, cp. Figure 3. It comprises the same type of microcontroller, IMU and wifi module as within the belayer setup.

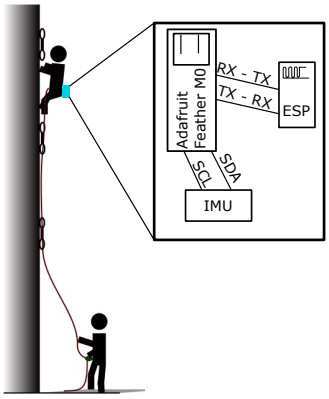

Figure 2 Sketch of the electronical components attached on the harness of the climber. They consist of a circuit board including a microcontroller, SD card socket, wifi module and an IMU.

2.3 Wireless Synchronization

The information from the device on the climber contains the label information for the fall classification task. Therefore, the two devices had to record the sensor information synchronous. In order to comply with this requirement, we sent a signal via wifi broadcast message to both devices. The synchronisation rate of 1/minute guaranteed a time drift of less than one millisecond throughout the recorded sequence.

3 Measuring Setup

This section provides an overview of the measuring setup and the recording configurations. As we are interested in identifying falls in climb scenarios, we established two independent setups. The isolated fall sequences record climbing falls. The climb sequences provide information about climb specific movements and activities without any falls. Figure 3 displays the two configurations.

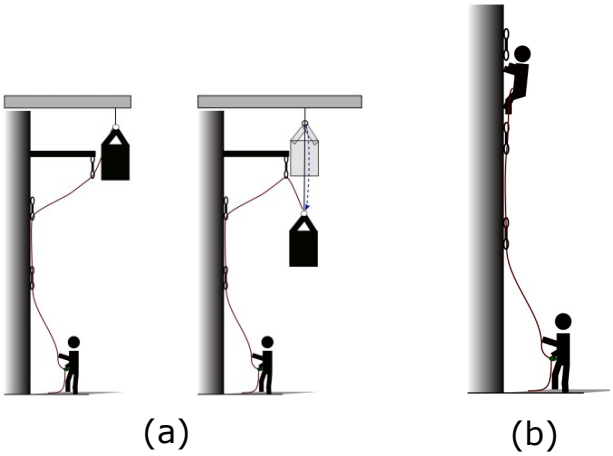

Figure 3 Sketch of the measuring setups for fall (a) and climb (b) scenarios. In case of the fall scenario a sandbag served as a substitute for the climber.

3.1 Isolated Fall Sequences

We recorded isolated fall sequences by using a sandbag as a substitude for the climber, cp. Figure 3 (a). This allowed us to record falls with a fall distance of over three to four meter without endangering the climber. Figure 4 displays such a conducted fall in terms of the recorded signals. This allows us to analyze the falls by identifying the starting time of the free fall, the fall into rope or the rope running through the device, and also to identify the movement behavior of the belay device itself.

Overall, we recorded 161 falls with varying configurations. Table 1 summarizes the falls with respect to the two variables *slack* and *fall potential*. Slack refers to the amount of loose rope handed out by the belayer, whereas fall potential defines the height difference between the rope attachment point on the climber and the last clipped quickdraw, cp. Figure 5. Both configurations share the same fundamentals by affecting the free fall time of the climber. Though, slack is additionally influenced by the friction caused by the rope running through the quickdraws. On the other side, the impact of the climbers' fall into the rope appears higher if the fall potential increases.

The amount of slack and fall potential differ in some configurations. For example, in Setup 2, the amount of

ISBN 978-3-8007-5835-7

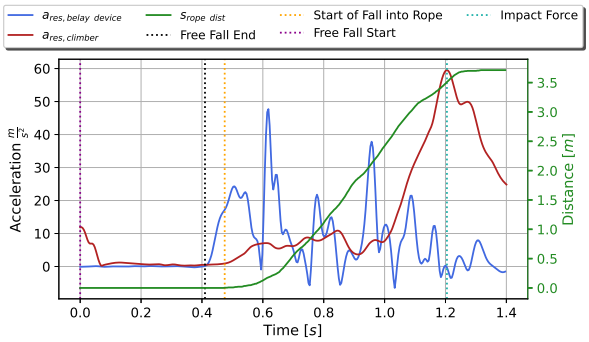

Figure 4 Fall example from a sandbag drop with one meter of slack. The graphic displays the measured distance of rope running through the belay device (green), the resulting acceleration measured on the climber (red) and belay device (blue). It also depicts the timestamps of releasing the sandbag (violet), the occurring impact force (turquoise), the end of the free fall (grey) and the starting point of the rope running through the device (orange).

slack was $0.35\,m$. This was the natural amount of slack the belayer was able to pull out, and, hence serves as a comparable reference against the climb scenarios, cp. Section Climb Sequences. Likewise, the same is applicable to the slack of $0.7\,m$, where the belayer pulled out rope twice.
The rest of the configuration values are $0.25\,m$, $0.5\,m$ and $1.0\,m$. As we recorded multiple belayer, those values serve as a normed reference in-between those belayer.
Finally, we varied the handling of the belay device, to analyze its movement behavior in three different handling situations: holding the device, the carabiner or nothing.

Table 1 Setup of the recorded fall configurations. Variations in fall potential and slack were chosen to depict the reality as close as possible.

Setup Number	Belay Device Handling	Number of Recordings	Slack $[m]$	Fall Potential $[m]$
1	Device	42	0.00	0.00
2	Device	3	0.35	0.00
3	Device	10	0.50	0.00
4	Device	4	0.70	0.00
5	Device	10	1.00	0.00
6	Device	13	0.00	0.25
7	Device	19	0.00	0.50
8	Device	7	0.00	1.00
9	Device	5	0.35	0.25
10	Carabiner	5	0.00	0.00
11	Carabiner	5	0.70	0.00
12	Carabiner	5	0.00	1.00
13	Carabiner	5	0.70	1.00
14	Nothing	12	0.00	0.00
15	Nothing	3	0.35	0.00
16	Nothing	1	0.50	0.00
17	Nothing	3	0.00	0.25
18	Nothing	6	0.00	0.50
19	Nothing	3	0.00	1.00

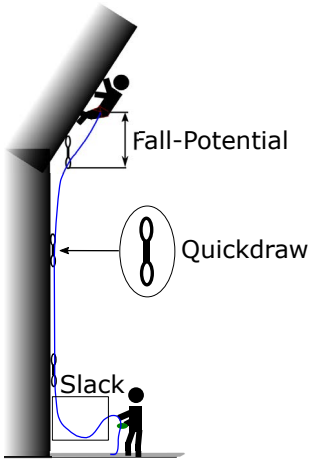

Figure 5 Configurations for the fall setup. Fall configuration describes the height difference of the climber to the last clipped quickdraw. Slack refers to the amount of loose rope handed out by the belayer. It can be described as the amount of rope which is required to pull in until the rope is straightened between the belay device and the first clipped quickdraw without considering the strain of the rope.

3.2 Climb Sequences

The second setup aims to record climb sequences that occur in real climb scenarios. Overall, we conducted 45 recordings based on 6 different configurations, as seen in Table 2.
Within the fall configurations, it was possible to adjust the slack precisely. This is not feasible for the climb sequences, as our aim was to create a natural climbing environment. So, we only differentiated between slack and no slack, referred to as "Yes" and "No" respectively. A second configuration parameter is the position from which the climber clips into the next quickdraw. We examined two options: one, where the quickdraw is one arm length away from the climber (Long Arm) and one, where the quickdraw is located at the height of the chest of the climber (Chest Height). The first configuration requires the belayer to pull more rope through the device than the second one.
Thirdly, the belayer was allowed to either belay actively or passively. In the active situation, the belayer moves in rope direction whilst the climber is demanding for rope. The passive belaying activity requires the belayer to stand still in this situation.

Table 2 Setup of the recorded climb configurations. Slack, clipping position and belayer activity were varied.

Setup Number	Number of Recordings	Belayer Activity	Clipping Position	Slack
1	7	Passive	Chest Height	No
2	8	Active	Chest Height	No
3	8	Passive	Long Arm	No
4	7	Active	Long Arm	No
5	7	Passive	Chest Height	Yes
6	8	Passive	Long Arm	Yes

ISBN 978-3-8007-5835-7

4 Signal Processing

This section provides an overview over the individual channels and explains the methods to pre-process and analyse the recorded signals.

4.1 Inertial Measurement Unit

From the 9 axis Motion Processing Unit, we recorded the information from the three axis accelerometer and three axis gyroscope. The acceleration signal was filtered using a low pass butterworth filter of fourth order with a cutoff frequency of $30\,Hz$. In combination with the information obtained by the gyroscope we used the Madgwick orientation filter [10] with a divergence rate of $\beta = 0.8$ to rotate the local coordinate frame of the IMU to align with earth's frame. This way, we are able to subtract the gravitational influence in the following way:

$$\vec{a} = \vec{a}_r - (0,0,g)^T$$

, with g as the gravitational constant and $\vec{a}_r$ the acceleration reading from the sensor, rotated into the earth frame.

4.2 Hall-Sensor

The three Hall-Sensors allowed us to keep track of rope running through the belay device. They are placed in a 40° angle in between them. As the sensors have to interact with magnets to keep track of the rope, we integrated six of them in a wheel, which was pressed against the rope itself, cp. Figure 1. The magnets are placed 60° apart with changing poles. As the radius of the wheel is around $r_{Wheel} = 0.012\,m$, the sensitivity of the measurable rope distance is around $r_{Rope,Sensitivity} \approx 4.1\,mm$.

4.3 Sequencing

In addition to pre-processing the raw information from the sensors, we had to cut the recorded trials to remove the non-informative time ranges (the time right before the fall was initiated and the time before the climber started to climb the wall).
For cutting the fall trials, we identified the moment of release based on the signals from the climber. They mark the starting point of the time sequence. The impact force was defined as end point as further time steps do no account as a fall.
The initial time the rope was pulled through the device marks the starting point for the climb trials. Lowering was included into the sequences and around the time the climber reaches the floor, the recording stopped.

4.4 Hardware Requirements

The fall of a climber is a time critical event. According to the Norm EN892 a rope has to withstand a certain amount of falls with a fall factor of 1.77. This would result in a fall with a fall potential of $2.3\,m$ and an additional amount of slack of about $0.3\,m$. Based on the properties of the wheel and magnets interacting with the Hall-Sensor, such a fall would require to trigger each Hall-Sensor every $440.88\,\mu s$. Our Interrupt Service Routines (ISR) require at max $90\,\mu s$ of time, hence never facing the issue of missing out an event.
The average time of our recorded falls took around $1.2\,s$ until the impact force occured. So, we recorded and stored the data with a frequency of about $220\,Hz$.

5 Data Analysis

This section provides a brief summary about the sample and feature space, the analysis of the data and the algorithms applied to handle the classification task.

5.1 Preparation of the Sample and Feature Space

The feature space is built around the sensor components described in Section 2. From those, we extracted seven features: the three axes from the accelerometer, the three axes from the gyroscope and the velocity information of the rope running through the belay device. We chose the velocity, as the distance of the rope would unambigously lead to an easy identification of a fall, as climb sequences lead to traveled rope distances of above $20\,m$. A fall sequence on the other hand results in measured distances of less than $5\,m$. Additionally, the climbed distance feature contains a time dependency. Meaning, the higher the climber climbs a climbing route, the further the distance measured. The velocity is able to compensate this dependency, as it is defined as the gradient of the distance with respect to the time.
The velocity was calculated first by applying an average filter with a filter size of 15 samples on the distance feature. After the filter was applied, we estimated the velocity v based on the forward difference approximation:

$$v(t+\Delta t) = \frac{s_{rope}(t+\Delta t) - s_{rope}(t)}{\Delta t}$$

The raw information from each of the seven features was then transformed into their respective SI-unit and then standardized to equalize their means and establish a unit-variance.
The temporal information was neglected in this study. So, each sample represents one time step.

5.2 Class Separability

In Figure 6, a pairwise feature plot, where each axis is representing one of the seven features, is depicted. The utilized abbreviations in this graph are A and G for the acceleration and angular velocity. The second letter X, Y and Z represents the direction, in which the kinematics were measured. Due to the high amount of data and scattering in between them, we applied a 2D hexagon binning plot with at least 150 samples per hexagon. This allows us to analyze and compare the cluster center among the two classes. We can see a high overlap between the two centers. Therefore, they are difficult to be distinguished in the 2D feature space.

ISBN 978-3-8007-5835-7

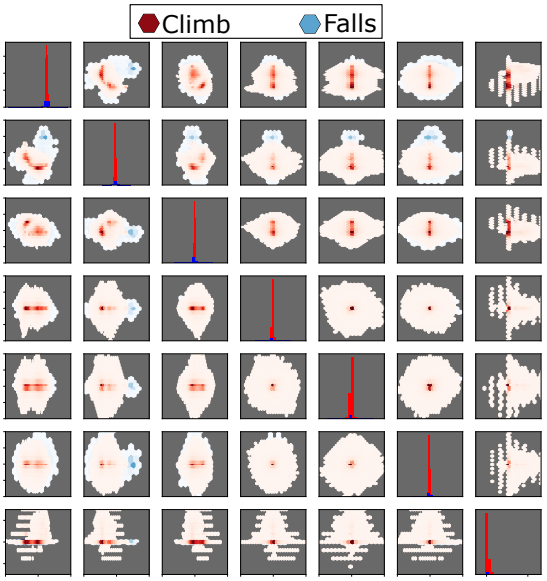

Figure 6 Pairwise feature plot of the applied features. Each graph in the upper and lower triangular matrix is generated as 2D hexagon binning plot where at least 150 samples are required for a hexagon to be visualized. The more intense the color, the more samples are within this specific hexagon. Diagonal entries represent a histogram of the respective feature.

Instead of the visual inspection for the data separability, we can use a density approach to identify the amount of overlap between the two classes, even in the full feature space. Therefore, we used a Gaussian Mixture Model with one component to identify the threshold of the density, where 99 % of the climb samples lie. Within this area, we could identify 57.86 % of the fall samples to be within this area.

6 Classifier

We were analyzing three approaches to classify a climbers fall. The first one utilizes a threshold on the velocity of the rope running through the device. We used a threshold of 4 $\frac{m}{s}$, similar to the REVO belay device from the Wild Country Ltd company (Derbyshire, SK17 8PY, United Kingdom), which is capable of blocking the rope movement at the same speed. Though, the blocking of the rope is enabled by a mechanical mechanism. In the following, we call this method "threshold method".
The second approach is based on the Random Forest method [11]. We set the number of trees to 200 and allowed a maximum depth of 4 per tree. For the split criteria, we relied on the Gini impurity.
Finally, the last evaluated approach is a combination of both methods. We used the velocity information to pre-process the input data even further by neglecting samples with a velocity of zero. Random Forest is, again, the classifier to handle the differentiation task. The configuration is identical to the aforesaid Random Forest approach.

7 Results

This section provides the results from the study to classify a climbers fall based on kinematic sensor information generated with the belay device. The three classification approaches will be analysed separately.

7.1 Threshold Method

The two sample distributions of the individual classes are visualized in Figure 7. Fall samples (left box-plot) show a higher dispersion with a standard deviation of around 2.55 $\frac{m}{s}$, compared to the climb samples (middle box-plot) with a standard deviation of 0.37 $\frac{m}{s}$. Fall potential and slack are the cause for reaching high velocity values, and, hence increasing the dispersion. We recorded velocities of up to 11.92 $\frac{m}{s}$. Even the third quartile lies above the threshold with a value of 4.16 $\frac{m}{s}$. Compared to that, climb samples reach a maximum velocity of 4.32 $\frac{m}{s}$, which also exceeds the threshold. Though, the third quartile is equal to zero, showing that most samples were not recorded while handing out rope. It is also the only class registering negative velocities. They occur when the belayer is pulling rope in.
The right box-plot (Max-Velocity Falls) displays the maximum reached velocities within each fall sequence. With a minimum value of 4.54 $\frac{m}{s}$, which is above the threshold, it shows that at least once per fall sequence a sample is correctly classified.
The full classification result is displayed in the confusion matrix in Figure 8 (a). With a specificity of about 99.9983 %, only 24 samples were falsely classified as falls. Though, the sensitivity is dropping to 27.17 %. Overall, we reached a geometric mean of 52.11 %.

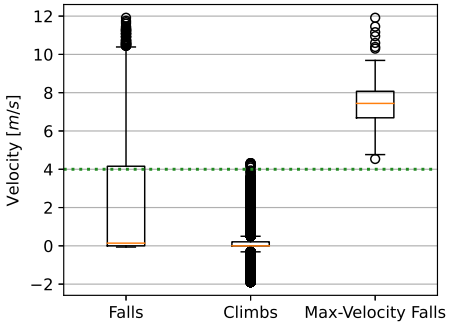

Figure 7 Class individual distributions (Falls and Climbs) of the velocities from the rope running through the belay device. The green dotted line represents the threshold of 4 $\frac{m}{s}$. The maximum velocities per fall sequence is visualized as well (Max-Velocity Falls). It displays that at least one sample within each fall sequence is being classified correctly as a fall.

Threshold Method

19874	53279	Sensitivity 27.17 %
24	1375025	Specificity 99.9983 %
Precision 99.88 %	Neg. Predicted Value 96.27 %	Geometric Mean 52.11 %

(a)

Random Forest Method

32602	40551	Sensitivity 44.57 %
1285	1373764	Specificity 99.91 %
Precision 96.21 %	Neg. Predicted Value 97.13 %	Geometric Mean 66.73 %

(b)

Combined Method

28681	9825	Sensitivity 74.48 %
792	385501	Specificity 99.79 %
Precision 97.31 %	Neg. Predicted Value 97.51 %	Geometric Mean 86.21 %

(c)

Figure 8 Results of the classification with the threshold (a), the Random Forest (b) and the Combined method of the two approaches (c). The threshold reaches a geometric mean of 52.11 % with 24 false positives samples and a sensitivity of 27.17 %. The Random Forest approach reaches a sensitivity of 44.57 % and 1285 false positives which leads to a geometric mean of 66.73 %. Sensitivity and geometric mean improved with the Combined method by reaching values of 74.48 % and 86.21 % respectively. Only the specificity dropped to 99.79 %.

7.2 Random Forest Method

The tree based classification algorithm is able to improve the results with respect to the geometric mean and sensitivity, cp. Figure 8 (b). We receive a sensitivity of 44.57 % and a geometric mean of 66.73 %. The benefit of improvement drops the specificity by 0.08 % which accounts for more than 1200 additional false positives.

7.3 Combined Method

The velocity also serves as an indicator of how often the rope is being handed out. In a climb scenario, a belayer hands out rope in 29.61 % of the time, whereas in our recorded falls 52.68 % of the time rope was registered running through the device. This bias might influence the outcome of the prediction results. By neglecting samples with a velocity of zero in both classes, we wanted to decrease the initial bias. It lead to an improvement of the sensitivity to 74.48 % with a decreasing specificity to 99.79 %. As the amount of overall samples declined, the false positives decreased as well to 792, despite a lower specificity.

8 Discussion

The recent popularity in sport climbing lead to an increase in injury reports. Therefore, we developed a monitoring system and analyzed the falls of a climber. It consists of two sub-systems, one, integrated into a belay device, and the other one generating the required label information in fall situations, which is attached to a climber or a substitute.

Even with the more simple threshold method, we were able to identify at least one sample per trial correctly as a fall. Though, we did not analyze the time until a fall would be identified as such. This is a critical variable and requires to be as fast as possible to decrease the covered height of the fall. The random forest approach, especially in combination with the velocity information improves the sensitivity which might improve the time of the catch. It is still an ongoing investigation and needs to be analyzed in more detail.

The specificity seems to be very high at 99.9983 % in the case of the threshold method, though, no climber would rely on a belay device which blocks rope movement too often in climb typical situations like handing out rope. So, further improvements have to be done by reducing the false positives, especially, when relying on machine or deep learning methods.

Machine learning methods prefer the majority class in a skewed dataset. As our dataset is affected by a class imbalance, we can see such a preference towards the climb class when using the random forest approach. Though, balancing out the classes within the dataset could lead to a deterioration of the majority class. So, it depends on the question that needs to be clarified to what extend the skewed dataset is to be balanced.

In this study we neglected the temporal information. So, each sample represented one time step. In case of a fall, we would assume the device to be pulled upwards, before any rope is running through the device, which is not supposed to be the case whilst handing out rope. This information could be beneficial for the classification task and would require to add temporal information.

9 Conclusion and Outlook

This study showed the possibility for a monitoring system in sport climbing, which is integrated directly into a belay device. We recorded the movement behavior of the device with an IMU and the amount of rope running through it with Hall-Sensors. With the help of wireless communication between the components in the belay

device and one attached to the climber, we were able to generate a data set with label information for predicting falls in sport climbing. Three classification approaches were analyzed. The first one is based on a threshold, the second on the Random Forest method and the third is a combination of both. The threshold approach is able to achieve a very high specificity with only 24 false positive samples. With a sensitivity of less than 30 %, it is still able to identify at least one sample within each trial as a fall.

Best results, in the sense of geometric mean, were achieved by combining the velocity information with the random forest approach. We reached a value of 86.21 %. In this scenario, the specificity was dropping to 99.79 % with 792 false positives. The sensitivity was increasing by almost 50 % compared to the threshold variant.

The dataset shows a class imbalance, where 5.05 % of the samples belong to the fall trials. Due to the nature of the approach, the threshold method is not affected by this imbalance. Though, even the random forest method was able to handle it by a certain degree. One explanation arises through the different type of sequences during a climb trial, as only 29.61 % of all climb samples hold information about rope movement. Future work could improve the classification results by including this information and separating the classes even further.

Future work also has to be done by analyzing the influence of the temporal information. We were still able to achieve a geometric mean of over 86 %. Though, relying on the temporal information could not only improve the classification result but also lead to a faster identification of a fall. The biggest improvement in this direction might be to identify a fall before any rope is even running through the device itself.

Funding

This project was funded by the Federal Ministry for Economic Affairs and Energy (BMWi) and their Central Innovation Programme (ZIM) for small and medium-sized enterprises (SMEs) under the funding indicator ZF4137908RP8.

Acknowledgments

We acknowledge the Edelrid GmbH & Co. KG for their support and contribution throughout this research project.

Literature

[1] N. G. Nelson and L. B. McKenzie, "Rock climbing injuries treated in emergency departments in the u.s., 1990-2007," vol. 37, pp. 195–200, 2009.

[2] V. R. Schöffl, G. Hoffmann, and T. Küpper, "Acute injury risk and severity in indoor climbing-a prospective analysis of 515,337 indoor climbing wall visits in 5 years," *Wilderness & environmental medicine*, vol. 24, no. 3, pp. 187–194, 2013.

[3] J. Boulanger, L. Seifert, R. Herault, and J.-F. Coeurjolly, "Automatic sensor-based detection and classification of climbing activities," *IEEE Sensors Journal*, vol. 16, no. 3, pp. 742–749, 2016.

[4] A. Bonfitto, A. Tonoli, S. Feraco, E. C. Zenerino, and R. Galluzzi, "Pattern recognition neural classifier for fall detection in rock climbing," *Proceedings of the Institution of Mechanical Engineers, Part P: Journal of Sports Engineering and Technology*, vol. 233, no. 4, pp. 478–488, 2019.

[5] C. Ladha, N. Y. Hammerla, P. Olivier, and T. Plötz, "Climbax," *UbiComp 2013 - Proceedings of the 2013 ACM International Joint Conference on Pervasive and Ubiquitous Computing*, pp. 235–244, 2013.

[6] A. Tonoli, R. Galluzzi, E. C. Zenerino, and D. Boero, "Fall identification in rock climbing using wearable device," *Proceedings of the Institution of Mechanical Engineers, Part P: Journal of Sports Engineering and Technology*, vol. 230, no. 3, pp. 171–179, 2016.

[7] H. Oppel and M. Munz, "Analysis of feature dimension reduction techniques applied on the prediction of impact force in sports climbing based on imu data," *AI*, vol. 2, no. 4, pp. 662–683, 2021.

[8] Infineon Technologies, "Uni- and bipolar hall ic switches for magnetic field applications." November 2007.

[9] InvenSense Inc., "Mpu-9250 product specification revision 1.1." June 2016.

[10] Sebastian O.H. Madgwick, Andrew J.L. Harrison, Ravi Vaidyanathan, "Estimation of imu and marg orientation using a gradient descent algorithm," *2011 IEEE International Conference on Rehabilitation Robotics*, pp. 1–7, 2011.

[11] LEO BREIMAN, "Random forests," *Machine Learning*, no. 45, pp. 5–32, 2001.